C6 pyridinium ceramide influences alternative pre-mRNA splicing by inhibiting protein phosphatase-1

Chiranthani Sumanasekera[1], Olga Kelemen[1], Monique Beullens[2], Brandon E. Aubol[3], Joseph A. Adams[3], Manjula Sunkara[1], Andrew Morris[1], Mathieu Bollen[2], Athena Andreadis[4] and Stefan Stamm[1],*

[1]Department of Molecular and Cellular Biochemistry, University of Kentucky, Lexington, Kentucky 40536, USA, [2]Laboratory of Biosignaling and Therapeutics, Department of Molecular Cell Biology, University of Leuven, B-3000 Leuven, Belgium, [3]University of California, San Diego La Jolla, CA 92093 and [4]UMASS Medical School, 55 Lake Avenue North, Worcester, MA 01655-0106, USA

ABSTRACT

Alternative pre-mRNA processing is a central element of eukaryotic gene regulation. The cell frequently alters the use of alternative exons in response to physiological stimuli. Ceramides are lipid-signaling molecules composed of sphingosine and a fatty acid. Previously, water-insoluble ceramides were shown to change alternative splicing and decrease SR-protein phosphorylation by activating protein phosphatase-1 (PP1). To gain further mechanistical insight into ceramide-mediated alternative splicing, we analyzed the effect of C6 pyridinium ceramide (PyrCer) on alternative splice site selection. PyrCer is a water-soluble ceramide analog that is under investigation as a cancer drug. We found that PyrCer binds to the PP1 catalytic subunit and inhibits the dephosphorylation of several splicing regulatory proteins containing the evolutionarily conserved RVxF PP1-binding motif (including PSF/SFPQ, Tra2-beta1 and SF2/ASF). In contrast to natural ceramides, PyrCer promotes phosphorylation of splicing factors. Exons that are regulated by PyrCer have in common suboptimal splice sites, are unusually short and share two 4-nt motifs, GAAR and CAAG. They are dependent on PSF/SFPQ, whose phosphorylation is regulated by PyrCer. Our results indicate that lipids can influence pre-mRNA processing by regulating the phosphorylation status of specific regulatory factors, which is mediated by protein phosphatase activity.

INTRODUCTION

All polymerase-II transcripts undergo pre-mRNA processing and at least 95% of the transcriptional units are alternatively spliced (1). The exact regulation of alternative splicing events is physiologically important, as evidenced by an increasing number of diseases that are caused by the selection of the wrong splice site (2). The proper recognition of exons is regulated by the transient formation of protein complexes on the pre-mRNA that identify a sequence for its recognition by the spliceosome. The signals on the pre-mRNA that mark an exon for its inclusion in the mRNA are highly degenerate, most likely to avoid interference with coding requirements. Therefore, exons are recognized by the formation of a complex between the pre-mRNA and various hnRNPs and SR proteins. Since these proteins generally bind to RNA with low selectivity, a higher specificity is achieved by simultaneous binding of the proteins to each other.

The interaction between these proteins is regulated in part by their phosphorylation status. For example, protein phosphatase-1 (PP1)-mediated dephosphorylation promotes the interaction between Tra2-beta1 and SF2/ASF (also called SRSF1) *in vitro* (3). Reversible phosphorylation of SR proteins and hnRNPs is achieved by an interplay between protein kinases and phosphatases. Several SR proteins contain an evolutionarily highly conserved PP1 binding element (RVxF) in their RNA recognition motif which allows PP1 to influence the phosphorylation status of proteins bound to pre-mRNA. In addition to the interaction between individual SR proteins, the affinity between components of the spliceosome, such as U1-70K and proteins that associate with pre-mRNA, including PSF/SFPQ (4), SRp38 (5) and

SF2/ASF (6) is influenced by their phosphorylation status. This suggests that PP1 activity can regulate the recognition of pre-mRNA substrates by the spliceosome and influences the selection of alternative exons by altering protein affinities. In agreement with this model, a change in PP1 activity has been shown to alter splice site selection *in vivo* (3,7,8).

Ceramides are a class of sphingolipids that are composed of sphingosine and a fatty acid moiety. In the cell, ceramide can be generated by sphyingomyelin hydrolysis by sphingomyelinase or by *de novo* synthesis. Sphingomyelin and sphingomyelinase are both present in the nucleus, which led to the suggestion that they participate in nuclear signaling (9). Natural ceramides contain long alkyl groups (C14–26) and are therefore hydrophobic. It has previously been shown that endogenous ceramides alter bcl-x splicing via a purine-rich splicing enhancer (10). To improve delivery and water solubility, cationic-ceramide analogs containing pyridinium moieties were synthesized. Owing to their ability to induce apoptosis, these water-soluble ceramide analogs have been tested as anti-cancer drugs (11,12). Despite their usage in clinical studies, the effect of these pyridinium ceramides on alternative splicing has not been determined.

Here, we investigate the role of a water-soluble ceramide analog, C6 pyridinium ceramide (PyrCer), in alternative splicing. We found that PyrCer treatment inhibits the dephosphorylation of splicing regulatory proteins by PP1, which is opposite to the activation reported for water-insoluble short and long-chain ceramides (13). In addition to SR proteins known to be affected by natural ceramides, PyrCer treatment increases the phosphorylation of other proteins involved in splicing, such as PSF/SFPQ, SAP155 and UAP56. It changes the alternative splicing patterns of exons that are short and dependent on splicing enhancers. These findings suggest that the dephosphorylation of splicing factors by PP1 is a molecular link between lipids and alternative splice site selection. The difference between PyrCer and natural ceramides suggest that subclasses of lipids have distincitve effects on splice site selection.

MATERIALS AND METHODS

Cell culture and transfection

HEK 293T cells were grown in DMEM (Invitrogen) supplemented with 10% (v/v) fetal bovine serum (Invitrogen) for 24 h to 80% confluence prior to ceramide treatment and to 60–70% confluence prior to calcium phosphate transfections. Transfection of the minigenes and RT-PCR analyses was performed as described (14).

Ceramide treatment

Four microliters of HeLa nuclear extract (Dundee Cell Products) was incubated in 1 mM MnCl$_2$ and 1× PNK buffer (70 mM Tris–HCl pH 7.6, 10 mM MgCl$_2$, 5 mM dithiothreitol). Twenty micromolar of C6 pyridinium ceramide (D-erythro-2-*N*-[6′-(1-pyridinium)-hexanoyl]-sphingosine bromide) (Avanti Polar Lipids), or 20 μM 1-(2-oxopropyl) pyridinium bromide (Sigma-Aldrich)

was added. After 5 min at 37°C, 4 μCi of [γ-^{32}P] ATP (7000 Ci/mmol, MP Biochemical) was added. The 50 μl reactions were then incubated for 30 min and the reaction was stopped by adding 6× SDS sample buffer (0.375 M Tris–HCl pH 6.8, 30% glycerol, 12% SDS, 12% 2-β mercaptoethanol and 0.075% bromophenol blue) followed by 10% SDS–PAGE. Proteins that were differentially phosphorylated in the ceramide lanes were excised from the gel and analyzed by MALDI TOF/TOF.

Minigene construction

Minigenes were constructed as described (14). The primers for the minigenes and the insert sequences are shown in Supplementary Figure S1.

Phosphatase assays

Hydrolysis of *p*-nitrophenylphosphate (*p*-NPP) was performed in 25 μl reactions containing 1× phosphate buffer (0.1 M sodium acetate, 0.05 M bis–Tris, 0.05 M Tris–HCl, 2 mM dithiothreitol, at pH 8.0), 50 mM *p*NPP, 1 mM MnCl$_2$ and 0.1 U of purified PP1 enzyme mix (Upstate, #14-110) at 37°C for 30 min. A PP1 unit releases 1 nmol of phosphate/min from 15 μM phosphorylase at 30°C. The reaction was terminated by the addition of 100 μl of 0.25 M NaOH and absorbance was measured at 410 nm. The activity of PP1 on Phosphorylase b was measured as previously described (15).

C6 pyridinium ceramide treatment of HeLa nuclear extracts

Ten micrograms of HeLa nuclear extract (NE) was incubated with 4 μCi [γ^{32}P] ATP for 30 min at 37°C in 1× PNK buffer (New England Bio Labs) plus or 10 μM C6 pyridinium ceramide in a 50 μl final volume. Radiolabeled-NE proteins were then subjected to immunoprecipitation overnight with 2 μg of indicated antibodies, 10 μl proteins A/G beads (Santa Cruz) and 200 μl RIPA-rescue buffer containing phosphatase and protease inhibitors. Immunoprecipitates were subjected to SDS–PAGE, proteins were transferred on to nitrocellulose membranes and analyzed by phosphor-imaging. The membranes were then blotted with the indicated antibodies for total protein expression. Representative ^{32}P signals and western blot results of triplicate experiments for SF2/ASF, Tra2-beta1, PSF, UAP56 and SAP155 are shown.

Protein expression and purification

Recombinant proteins were overexpressed in *Escherichia coli* BL21 (DE3) cells. Expression was induced with IPTG in a final concentration of 0.4 mM for 4 h at room temperature. The His-Tra2-beta1 protein and His-PSF protein were purified under denaturing conditions on Ni-NTA resin (QIAGEN). The cells were lysed in buffer #1 [20 mM Tris, 300 mM NaCl, 100 mM MOPS, 15% glycerol and 4 M guanidine hydrochloride pH (7.5)] using a French press. The cell lysate was clarified by centrifugation at 10 000 × *g* for 30 min at 4°C. The supernatant was incubated with Ni-NTA resin for 1 h at room

temperature. The resin was poured into a column and washed with buffer #1 containing 20 mM imidazole followed by washing steps with refolding buffers [buffer #1 containing decreasing concentration of GuHCl (pH 6.5)]. The proteins were eluted using buffer #5 [20 mM Tris–HCl, 300 mM NaCl, 100 mM MOPS, 15% glycerol (pH 2.2)].

GST-tagged SF2/ASF transformed *E. coli* cells were lysed in buffer A [50 mM Tris–HCl (pH 7.5), 300 mM NaCl, 0.5% Triton X-100, 0.1% 2-β mercaptoethanol, 1 mM DTT, 1 mM MnCl$_2$] using a French press. The supernatant was incubated with Glutathion sepharose 4B (GE Healthcare) beads for 2 h at room temperature. The slurry was packed into a column and washed with buffer B [50 mM Tris–HCl (pH 7.5), 150 mM NaCl, 1 mM DTT, 0.1% 2-β mercaptoethanol, 1 mM MnCl$_2$]. The protein was eluted with buffer C [100 mM Tris (pH 8), 10 mM glutathione] and was dialyzed against buffer D [50 mM Tris (pH 7.5), 100 mM NaCl, 1 mM MnCl$_2$, 1 mM DTT, 0.1% 2-β mercaptoethanol and 10% glycerol]. The proteins were stored at −80°C.

Dephosphorylation of purified Tra2-beta1-His$_6$

Seven micrograms of purified recombinant Tra2-beta1-His$_6$ bound to Ni-NTA beads (Qiagen) was phosphorylated in HeLa nuclear extract in the presence of 5 µCi [γ^{32}P] ATP for 30 min at 37°C in 1× PNK buffer. Beads were then washed with RIPA buffer and aliquoted into tubes containing the indicated amounts of PP1, C6 pyridinium ceramide, oxo-pyridinium, calyculin A or ethanol as indicated in a 30 µl volume containing 1× PP1 buffer. The dephosphorylation reactions were incubated for 30 min at 37°C and then boiled in SDS-sample loading buffer. Samples were resolved by SDS–PAGE and gels were coomassie stained and subjected to phosphor imaging. The ^{32}P signals and total protein in coomassie stained gels were used to determine the extent of Tra2-beta1 dephosphorylation.

Measurement of ceramides and sphingolipids by HPLC tandem mass spectrometry

Ceramides were quantitated by HPLC electrospray ionization tandem mass spectrometry using an ABI 4000 Q-Trap hybrid linear ion trap triple quadrupole mass spectrometer operated in multiple reaction monitoring (MRM) mode. Ion currents associated with lipid species specific precursor product ion pairs were determined as described by others with minor adaptations (16). In brief, lipids were extracted using acidified organic solvents (17), including 50 pmol C17 ceramide as a recovery standard. Ceramide molecular species were resolved using a 3 mm × 100 mm X-Terra XDB-C8 column (3.5 µm particle size, Waters, Milford, MA, USA) and a gradient of methanol/water/formic acid (61:39:0.5, v/v) containing 5 mM ammonium formate (solvent A) and acetonitrile/chloroform/water/formic acid (90:10:0.5:0.5, v/v) with 5 mM ammonium formate (solvent B) at a flow rate of 0.5 ml/min.

The instrument was operated in positive mode with optimal ion source settings determined empirically using a set of synthetic ceramides. MRM transitions monitored for the elution of ceramide molecular species were as follows: m/z 510 > 264, 14:0-Cer; m/z 538:264, 16:0-Cer; m/z 540:284, 16:0-DHCer; m/z 552:264, 17:0-Cer (internal standard); m/z 564 > 264, 18:1-Cer; m/z 566 > 284, 18:1-DHCer; m/z 566 > 264, 18:0-Cer; m/z 568 > 284, 18:0-DHCer; m/z 594 > 264, 20:0-Cer; m/z 596 > 284, 20:0-DHCer; m/z 624 > 284, 22:0-DHCer; m/z 650 > 264, 24:1-Cer; m/z 652 > 284, 24:1-DHCer; m/z 652 > 264, 24:0-Cer; m/z 654 > 284, 24:0-DHCer; m/z 680 > 264, 26:1-Cer; m/z 682 > 264, 26:0-Cer; m/z 708 > 264, 28:1-Cer; m/z 710 > 264, 28:0-Cer. Quantitation was accomplished by reference to standard curves generated using synthetic standards obtained from Avanti Polar Lipids (Alabaster AL) that were independently determined by accurate mass measurements. Measurements of C6 pyridinium ceramide and oxo-pyridinium were accomplished using the extraction method detailed above.

C6 pyridinium ceramide was separated using the chromatographic methods used for natural ceramides excepet that the MRM transitions monitored were m/z 476–379; 476–266 and 476–253. Precursor ion scanning experiments indicated that the m/z 379 species was derived by loss of the pyridinium group and the mz 266 and 253 species were derived by sequential loss of the hydroxy groups from the resulting ion. Oxo-pyridinium was separated by hydrophilic interaction chromatography using a 4.6 mm × 100 mm Luna HILIC column (3 mM particle size, Phenomenex, Torrance, CA, USA) with monitoring of MRM transitions m/z 136 > 93, m/z 136 > 79, m/z 136 > 65, m/z 137 > 57.

Immunoprecipatation and western blots

For immunoprecipitation (IP) of PP1 isoforms, HEK293T cells were grown to 70% confluencency in 6-well plates and transfected with 2 µg of EGFP-C2 vectors expressing PP1 alpha, PP1 beta, PP1 gamma or Tra2-beta1-RATA [constructs described in (3)]. After 12–14 h, cells were treated with 0 and 10 µM C6 pyridinium ceramide for 8 h before preparation of cell extracts. Cells were lysed for 30 min at 4°C in 200 µl of RIPA buffer (20 mM Na$_3$PO$_4$, 150 mM NaCl, 1% NP-40, 1% sodium deoxycholate, 5 mM 2-β mercaptoethanol, 0.1% SDS, 1 mM EDTA, 1 mM phenylmethylsulfonyl fluoride, 5 mg/ml of leupeptin, pepstatin A, antipain and aprotinin) supplemented with 75 U/ml Benzonase (Sigma-Aldrich). RIPA-Rescue buffer (10 mM sodium phosphate pH 7.2, 20 mM NaCl, and freshly added 1 mM dithiothreitol, 1 mM phenylmethylsulfonyl fluoride, and 20 mg/ml aprotinin) was added to each reaction to a final volume of 460 µl and subsequently 40 µl of pre-cleared 50% protein A sepharose CL-4 bead suspension (GE HealthCare) were added. The beads were washed once with 1 ml RIPA buffer and three times with RIPA-rescue buffer (10 mM sodium phosphate pH 7.2, 20 mM NaCl, and freshly added 1 mM dithiothreitol, and 1 mM phenylmethylsulfonyl fluoride) and were resuspended in a 60 µl final volume. Thirty microliters of these beads were used for western blotting while the remaining half was used for the HPLC assay.

RESULTS

C6 pyridinium ceramide (PyrCer) changes alternative splicing of endogenous genes

Ceramides have previously been implicated in regulation of splice site selection (7,8,18). However, the molecular mechanism of ceramide action on pre-mRNA processing is not clear, partly because ceramides are poorly soluble in water. We therefore concentrated on C6 pyridinium ceramide, a water-soluble ceramide analog which is currently being tested for the treatment of squamous cell carcinomas (19,20). To determine the influence of ceramide action on alternative pre-mRNA splicing, we used a medium-throughput RT-PCR screen (21) using RNA from HEK293 cells treated with C6 pyridinium ceramide.

First, we used HEK293 cells in an MTT cytotoxicity assay to determine a suitable concentration of PyrCer for this screen. As a control, we used oxo-pyridinium, a molecule that only differs from PyrCer by its propyl group that replaces the short chain ceramide moiety. Our data indicate that, at a $10 \mu M$ concentration, there was <5% cell death compared to higher concentrations of PyrCer which lead to >80% cell death following a 24 h treatment (Supplementary Figure S2). In contrast, increasing concentrations of oxo-pyridinium had no effect on cell viability. These data also indicate that the cytotoxicity of PyrCer is due to the ceramide group and not due to the cationic pyridinium group which results in its water solubility. Based on these studies, we treated cells for 24 h with $10 \mu M$ PyrCer and analyzed the changes in alternative splicing compared to oxo-pyridinium treatment.

In total, 92 alternative splicing events were tested and 29 splicing events showed a significant change in their alternative splicing patterns. We validated these 29 events by performing RT-PCR with mRNA extracted from HEK293 cells treated with or without $10 \mu M$ C6 pyridinium ceramide. From these, we selected five exons with the most significant changes for further analysis. These exons were present in the DRF1, TIAF1, POL-β, TAU and SYK pre-mRNAs. As shown in Figure 1, treatment with $10 \mu M$ PyrCer promoted both inclusion and skipping of exons. As a negative control, we validated the absence of a PyrCer effect on the pre-mRNAs of CCNE1, ECT2, SHC1 and STM1 genes which showed no change in the primary screen (Supplementary Figure S3). Similar to other signal-dependent splicing systems (22), exon inclusion differs around 10–20% between the treated cells and controls. However, these differences are statistically significant, with *P*-values from the student's test <0.01.

The alternative exon usage in the DRF1 (Dbf4-related factor 1) and POL-β (DNA polymerase beta) genes caused a frameshift in the encoded pre-mRNAs. Alternative splicing of the other exons in the TIAF1 (TGFB1-induced antiapoptotic factor 1), TAU (microtubule associated protein tau) and SYK (spleen tyrosine kinase) transcripts retained their reading frames. The inclusion of tau exon 10 has been shown previously to increase the affinity of the resulting tau isoform to microtubules and aberrant exon 10 usage results in frontotemporal dementia

(23). These data suggest that a treatment with PyrCer changes alternative splicing of several pre-mRNAs and could have functional consequences for the cellular proteome.

C6 pyridinium ceramide (PyrCer) changes alternative splicing of exons in a heterologous context

To determine whether the sequence elements that respond to PyrCer treatment are localized in the vicinity of the regulated exons, we introduced the alternatively spliced exons into reporter minigenes. We used a recently developed recombination technique that introduces the exon of interest between two constitutively spliced insulin exons (14). Depending on the intron length, the resulting reporter minigenes contained one to three exons cloned between the constitutive insulin exons. Their structures are schematically shown in Figure 2.

These reporter constructs were transfected into HEK293 cells and the cells were subsequently treated with C6 pyridinium ceramide. Total RNA was isolated and analyzed using minigene-specific primers. In all cases, we observed a C6 pyridinium ceramide-specific change that was congruent with the changes observed with the endogenous genes. However, the magnitude of the effect on exon usage was larger in the transfection studies, which was expected, as the reporter genes were overexpressed. As an additional negative control, we compared cells treated with the inactive Oxo-Pyr (Supplementary Figure S2) with naïve cells and found no effect on alternative splicing of the DRF1, TIAF1, POL-β, TAU and SYK pre-mRNAs (Supplementary Figure S4). The data suggest that C6 pyridinium ceramide-responsive sequences work in a heterologous context and reside in the alternative exons or their immediate flanking exons and introns.

C6 pyridinium ceramide (PyrCer) inhibits PP1

It has been previously reported that ceramides promote PP1 activity (13) and that exogenous D-(e)-C6-ceramide causes SR-protein dephosphorylation (24). We therefore tested whether the PyrCer has an influence on PP1 activity using the classical *p*-nitrophenyl phosphate phosphatase assay. An equimolar mixture of all three PP1 isoforms purified from rabbit was used as the PP1 source. As shown in Figure 3A, PyrCer blocks PP1 activity at $100 \mu M$ concentration, when 0.1 U PP1 are present. In contrast, oxo-pyridinium that represents the water-soluble moiety of PyrCer had no significant effect. We used calyculin A as a positive control for a PP1 inhibitor and found that it inhibits PP1 activity at a 10 nM concentration (Figure 3A and B). We next tested the influence of PyrCer on the natural PP1 substrate phosphorylase phosphatase and again found an inhibition starting from $25 \mu M$ (Figure 3C).

These data indicate that PyrCer inhibits PP1, although at a >1000-fold higher concentration than established phosphatase inhibitors like calyculin A or okadaic acid. Collectively, these data show that unlike C6 ceramide which activates PP1 and promotes SR protein
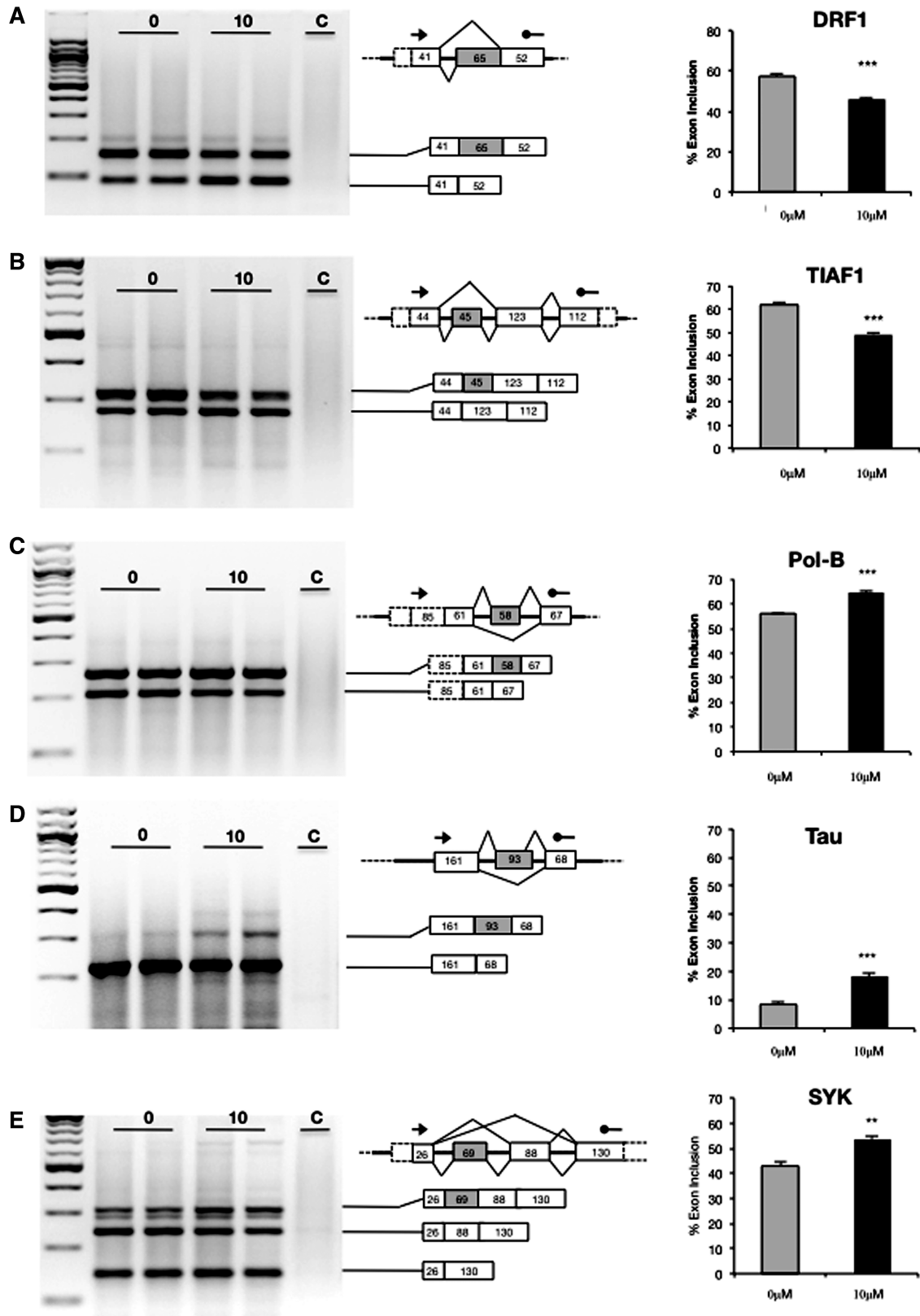
Figure 1. C6 Ceramide changes alternative splicing patterns of several endogenous genes. RT-PCR analyses of RNA from cells treated for 24 h with C6 pyridinium ceramide. Two representative examples of untreated and cells treated with 10 μM C6 pyridinium ceramide (PyrCer) are shown. The exon–intron structure of the regulated genes is indicated schematically next to the ethidium bromide stained gels. Numbers indicate the length of the exons. A statistical analysis of three independent experiments is shown on the right. The P values are (**A–D**) 0.0001 and (**E**) 0.001. The percent exon inclusion was calculated by dividing the intensity of the band representing the regulated exon with the combined intensity of all bands. C is a negative control without the reverse transcription. The regulated exons were: for DRF1 65 nt; TIAF1 45 nt; Pol-B: 58 nt; tau: 93 nt; SYK: 69 nt and are indicated in gray. Primers are indicated by arrows.
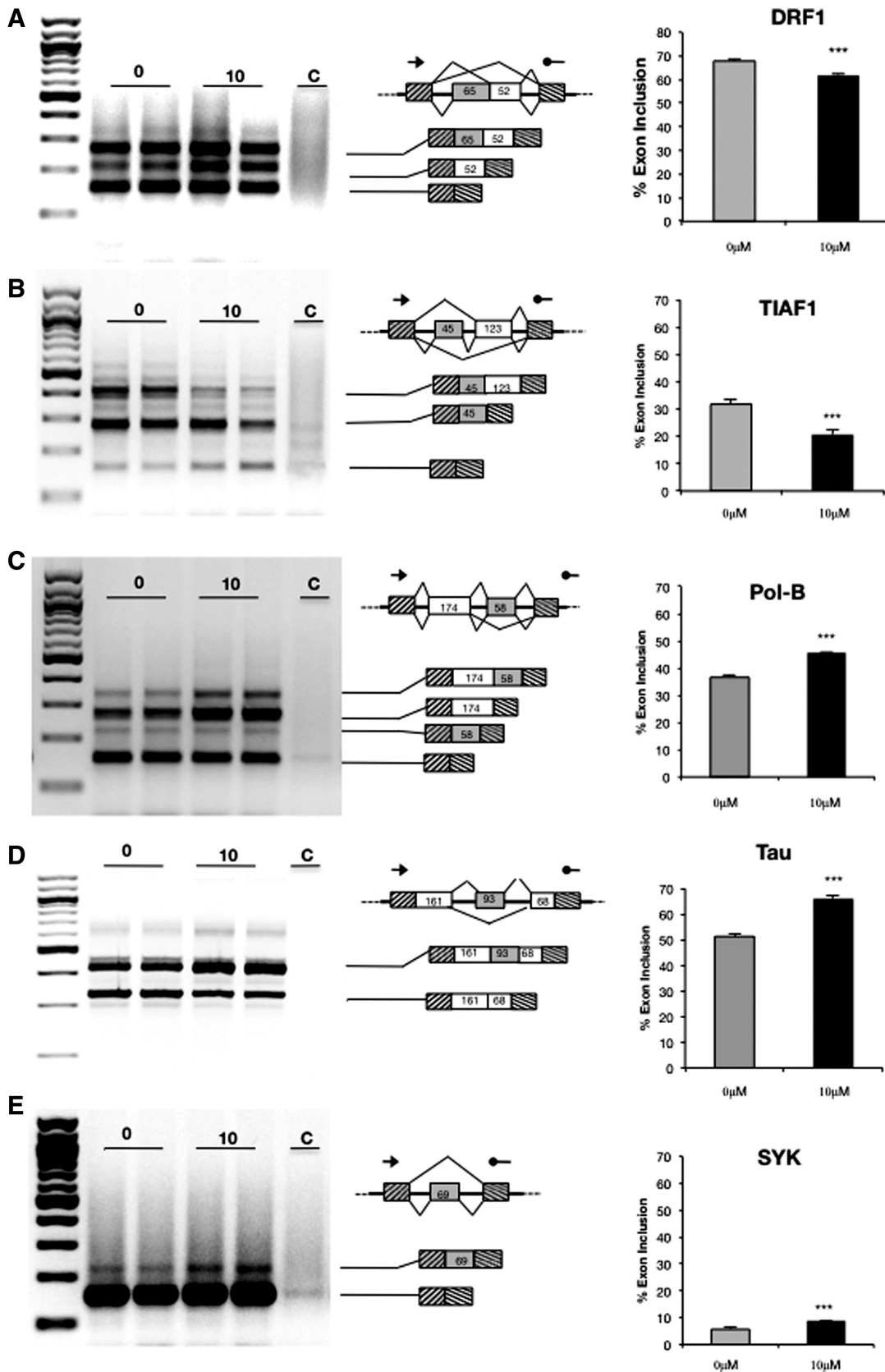
Figure 2. Reporter gene constructs recapitulate the effect of C6 pyridinium ceramide. The alternative exons regulated by C6 pyridinium phosphate were cloned between two constitutively spliced insulin exons into a heterologous splice reporter construct. One microgram of the constructs was transfected into HEK293 cells and the cells were treated with PyrCer for 24 h. Representative semi-quantitative RT-PCR analysis is shown. The statistical evaluation is shown on the right and was performed as described for Figure 1.
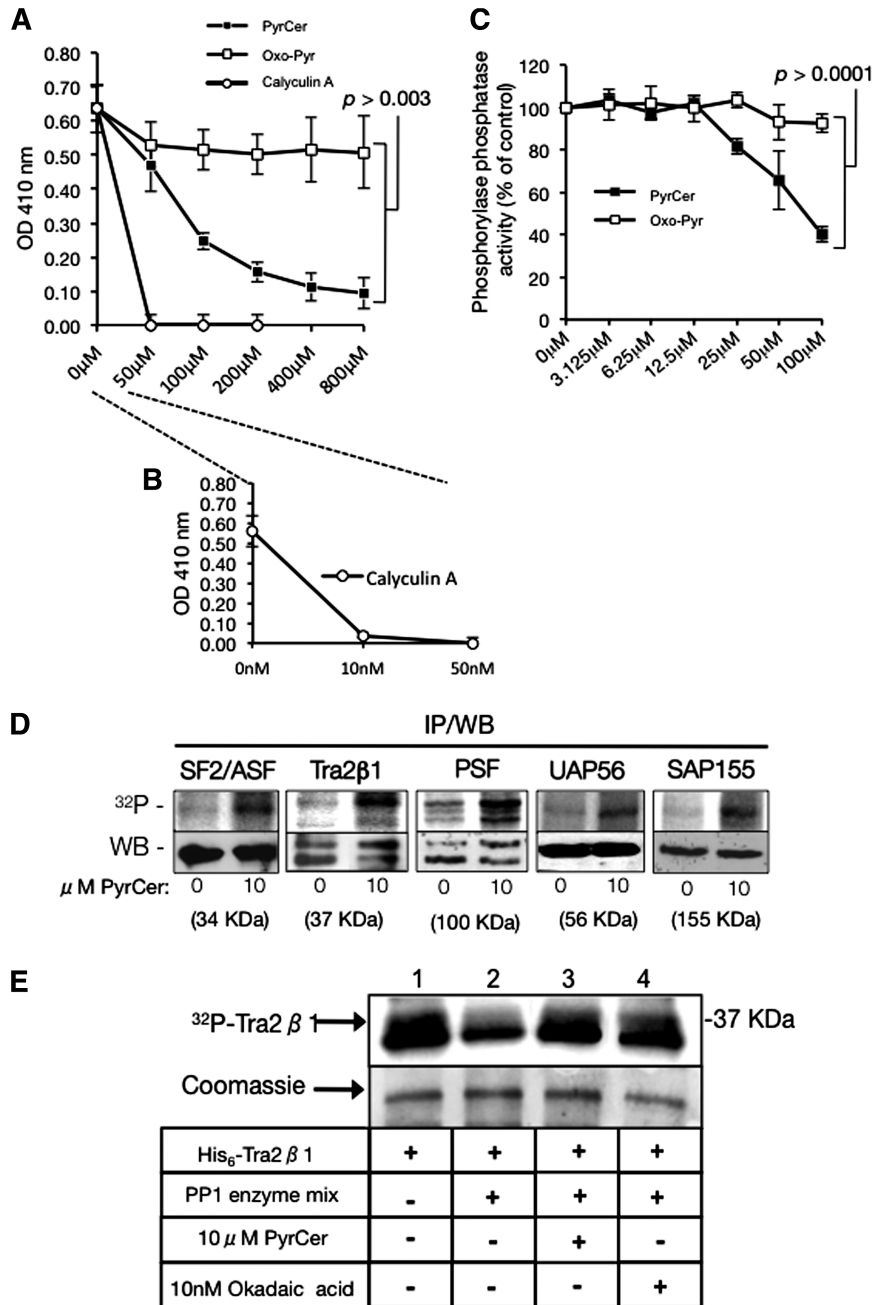
Figure 3. C6 pyridinium ceramide inhibits protein phosphatase-1. (**A**) An equimolar mixture of PP1 isoforms (alpha, beta and gamma) was incubated with the concentrations of C6 pyrimidinim ceramide indicated and the activity on *p*-nitrophenylphosphate was determined. 1-(2-Oxopropyl) pyridinium was used as a negative control. (**B**) The effect on the PP1/PP2A inhibitor calyculin A is shown for comparison. (**C**) PyrCer effect on PP1 dephosphorylating phosphorylase phosphatase. (**D**) PyrCer effect on the phophorylation of splicing factors. HeLa nuclear extract was incubated with [γ-^{32}P] ATP with or without 10 μM PyrCer and the proteins indicated were immunoprecipated. The top lanes (^{32}P) show the signal from overnight autoradiography. The signal form western blot using the antisera employed in immunorecipations are shown below. Tra2-beta1 and PSF migrate as doublet in western blots, which is due to different phosphorylation states (24). The numbers indicate the molecular weights. (**E**) Effect of 10 μM PyrCer on PP1-mediated dephosphorylation of purified Tra2-beta1 in vitro.

dephosphorylation (13) its water-soluble pyridinium analog, C6 pyridinium ceramide, inhibits PP1 activity.

C6 pyridinium ceramide treatment changes the phosphorylation of several splicing factors *in vitro*

Numerous nuclear proteins contain putative PP1 binding sites, and we recently showed that the splicing factors SF2/ASF, Tra2-beta1 and SRp30c (also called SRSF9) bind directly to PP1 using an evolutionarily conserved RVxF motif located in their RRMs (3). PSF/SFPQ is involved in several nuclear processes. It acts early in spliceosome assembly, is involved in transcriptional regulation and could play a role in homologous DNA recombination (26–28). Importantly, PSF/SFPQ contains a PP1 binding site in its RRM, which regulates its ability

to change alternative splicing (3,29,30). To determine whether PyrCer influences the phosphorylation of other nuclear proteins involved in splicing, we tested its effect on a splicing competent HeLa nuclear extract. We incubated HeLa nuclear extract with $4\,\mu$Ci $[\gamma\text{-}^{32}P]$ ATP in the presence or absence of $10\,\mu$M PyrCer and then subjected the reactions to SDS–PAGE. Proteins with a difference in phosphorylation signal were determined by autoradiography. The differentially phosphorylated bands were then identified by mass-spectrometry.

We next validated candidate genes by immunoprecipitation from extracts incubated with $[\gamma\text{-}^{32}P]$ ATP prior to the addition of $10\,\mu$M C6 pyridinium ceramide. The phosphorylation of the immunoprecipated proteins was detected by autoradiography and their general abundance was determined by by western blot. As shown in Figure 3D, PyrCer treatment increases the phosphorylation of SF2/ASF, Tra2-beta1, PSF/SFPQ, UAP56 and SAP155, but does not change overall abundance of these proteins. Again, this effect is opposite of the water-soluble C6-ceramide that promotes SF2/ASF dephosphorylation (24).

We previously showed that PP1 dephosphorylated Tra2-beta1 by binding to its RRM (3). As PyrCer inhibited Tra2-beta1 dephosphorylation in nuclear extracts, we tested if it could inhibit PP1-mediated dephosphorylation of the splicing factor when using recombinant proteins. His_6-tagged Tra2-beta1 purified from insect cells was ^{32}P-labeled and treated with $10\,\mu$M C6 pyridinium ceramide or $10\,$nM Okadaic acid in the presence or absence of $0.2\,$U of PP1. As expected, labeled Tra2-beta1 (Figure 3E, lane 1) was dephosphorylated by PP1 (Figure 3E, lane 2) but the presence of $10\,\mu$M C6 pyridinium ceramide inhibited the dephosphorylation of Tra2-beta1 by PP1 (Figure 3E, lane 3), similar to okadaic acid (Figure 3D, lane 4). Thus, PyrCer directly interferes with the dephosphorylation of a splicing factor by PP1.

Together, these data suggest that PyrCer treatment increased the phosphorylation of several splicing factors, which is likely caused by blocking PP1 activity. This effect is the opposite of the water-insoluble natural and short chain ceramides.

C6 Pyridinium Ceramide binds directly to PP1 *in vivo*

The inhibition of PP1 by PyrCer suggests that the two molecules interact with each other. To explore this interaction *in vivo*, we developed a mass-spectrometric assay for PyrCer detection. In brief, cells were treated with pyridinium ceramide for $24\,$h to allow PyrCer and PP1 to interact *in vivo*. Next, cells were washed and lysed, PP1-bound lipids were isolated with antibodies against PP1 and lipids were extracted from immune-complexes with chloroform, separated with HPLC and detected by ion trap triple quadrupole mass spectrometry (Supplementary Figure S5A). This method gives a linear response to PyrCer as shown in Supplementary Figure S5B and S5C. To test whether C6 ceramide binds to PP1 *in vivo*, we immunoprecipitated endogenous PP1 from cells that were treated with with or without $10\,\mu$M PyrCer using

a pan-PP1 antibody (Figure 4A and B). The ceramide signal obtained from the mass-spectrometry was normalized to the amount of PP1 present in the immunoprecipitations (Figure 4B).

We found that that PyrCer associates with PP1 *in vivo*. In addition, we performed a similar experiment with EGFP-tagged PP1 isoforms that were transfected into cells (Figure 4C). We immunoprecipitated the PP1 isoforms alpha and gamma using an antiserum against the GFP tag. As shown in Figure 4C, both isoforms bound PyrCer about equally. This interaction appears to be specific, as we could not detect C6 ceramide in immunoprecipites of Tra2-beta1-RATA, a Tra2-beta mutant that does not interact with PP1 (3) (Figure 4C). As a further internal control, we analyzed the presence of endogenous C18 ceramide in the immunoprecipitates. As
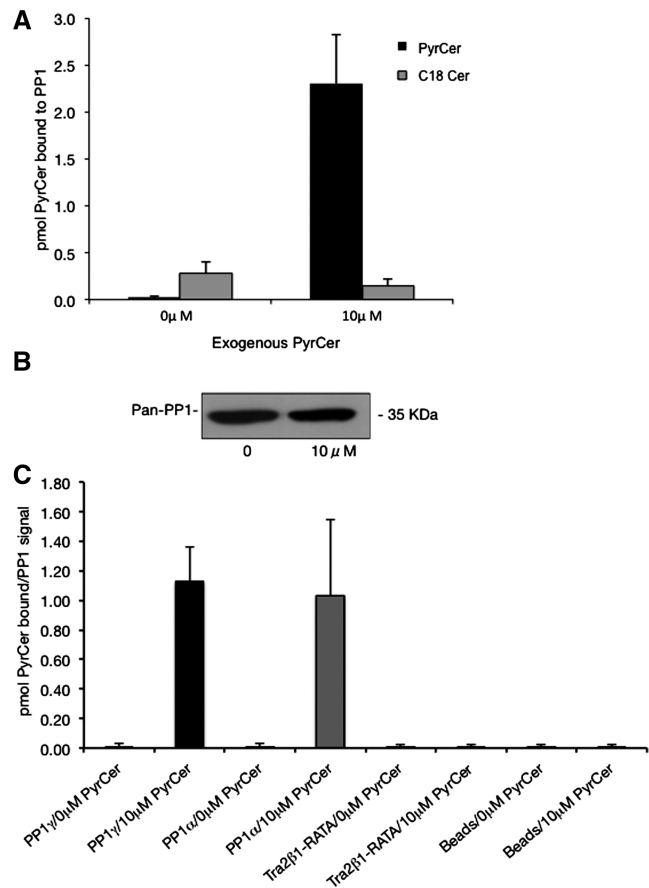

Figure 4. C6 pyridinium ceramide binds to protein phosphatase-1 in vivo. (**A**) Detection of PyrCer and C18 ceramide bound to PP1. HEK293 cells were treated with 0 and $10\,\mu$M C6 ceramide for $14\,$h and PP1 was isolated by immunoprecipitation with a pan-PP1 antibody. From the immunoprecipitates, bound lipids were extracted with chloroform and analyzed by mass-spectrometry. The mass-spectrometry signal was normalized to the amount of immunoprecipitated PP1, which was detected by western blot. The antiserum precipitates the catalytic subunit of PP1. (**B**) Detection of PyrCer bound to PP1 variants. (**C**) EGFP-tagged constructs expressing PP1 gamma, PP1 alpha, Tra2-beta1-RATA were transfected into HEK293 cells and immunoprecipitated with an anti EGFP antiserum. PyrCer bound to the immunoprecipitates was determined by mass-spectrometry and normalized to the signal obtained by western blot using anti EGFP.

shown in Figure 4A, C18 ceramide is associated with PP1 in untreated cells. However, the amount of C18 ceramide is reduced upon PyrCer addition, suggesting that both compounds might compete for the same binding site.

Finally, we determined whether PyrCer is taken up by cells or exerts its action by stimulating signal transduction cascades emenating from the cell membrane. We added 10 μM PyrCer to the cell medium and determined its intracellular distribution by cell fractionation. As shown in Supplemental Figure S6, about half of the lipid is accumulated in the cells after 24 h, with 40% in the cytosol and 10% in nuclear fractions. This argues that PyrCer can directly interact with cellular PP1 that is present in both the cytosol and nucleus.

In summary, these data show that cells take up C6 pyridinium ceramide, where it binds directly to PP1 and inhibits the phosphatase.

C6 ceramide responsive exons have common features

At a concentration of 10 μM, PyrCer changes alternative splicing of several exons *in vivo* (Figures 1 and 2). This could indicate that protein complexes forming around certain exons are more sensitive to PyrCer action and are changed at 10 μM concentration, which results in the preferential usage of another splicing pathway. To determine what features these exons have in common, we performed component analysis of the exons. All ceramide responsive cassette exons that we identified are shorter than the mammalian consensus length for cassette exons, which is around 150 nt. The mean length of the ceramide-responsive exons is 66 nt, with a SD of 20 nt (Supplemental Figure S7B). It is therefore likely that these exons depend on enhancer sequences to overcome their short length.

In order to determine common elements of PyrCer responsive exons, we performed MEME (Multiple Expectation matrices for Motif Elicitation) analysis of the sequences (31). We found that each PyrCer-regulated exon contains a GAAR and a CAAR motif (Supplemental Figure S7A). In addition, all exons contained SF2/ASF binding motifs predicted by ESE finder (32). The next common feature shared by all ceramide-responsive exons is suboptimal splice sites. The combined 3′ and 5′ splice sites flanking PyrCer-responsive exons have an average splice-site-strength score of 7.5, whereas the control constitutive exons have a score of 15, when calculated by a lod score algorithm based on mammalian splice sites (33) (Supplemental Figure S7C).

We next asked whether some of the regulated exons bind directly to PSF/SFPQ, SF2/ASF and Tra2-beta1, proteins that are dephosphorylated by PP1 and predicted to bind to PyrCer-reponsive exons. We purified PSF/SFPQ, SF2/ASF and Tra2-beta1 from bacteria and performed in vitro gel retardation assays using probes corresponding to the parts of POL-B and TIAF1 exons that contain the GAAR and CAAR motifs. As controls, we used arteficial oligonucleotides where these motifs were deleted. As shown in Figure 5, all three proteins bound to TIAF1 exon sequences. However Tra2-beta1 did not bind to the POL-B-exon RNA. This was surprising,

since the exon contains one AGAA binding motif that is the high affinity binding site for Tra2-beta1 (34). This suggests that an unknown sequence context contributes to Tra2-beta1 binding. The binding of Tra2-beta1, SF2/ASF and PSF to tau exon 10 has been reported earlier (35–37).

We conclude that C6 pyridinium-dependent alternative exons have suboptimal length, suboptimal splice sites and contain binding sites characteristic for splicing enhancers. It is therefore likely that their regulation is dependent on regulatory protein complexes that form on the pre-mRNA.

Splicing regulators with a PP1 binding site influence the regulation of C6 pyridinium ceramide responsive exons

We found that PyrCer treatment of HeLa nuclear extract caused an increase in the levels of phosphorylation of splicing factors PSF/SFPQ, SF2/ASF and Tra2-beta1 (Figure 3D). All these splicing factors are known to interact with PP1 (3). Therefore, we investigated the possibility that these splicing factors could effect splicing of the PyrCer-regulated exons.

As shown in Figure 6, the usage of all exons is changed by PSF. With the exception of the DRF1 pre-mRNA, PSF promotes exon skipping or inclusion of the tested reporter genes in a similar way as C6 pyridinium ceramide. SELEX experiments showed that PSF binds to sequences containing GAA-motifs (38) that are enriched in C6 pyridinium ceramide-responsive exons (Supplemental Figure S7A).

Bioinformatic analysis using ESE finder (32) indicates SF2/ASF binding sites in the regulated exons. Furthermore, all exons with the exception of DRF1 contain the high affinity Tra2-beta1 binding site AGAA. However, DRF1 contains the lower affinity Tra2-beta1 site TGAA. *In vitro*, Tra2-beta1 binds to AGAA and TGAA with 2.2 and 4.5 μM affinity, respectively (34). We therefore analyzed the ceramide-responsive minigenes in co-transfection experiments together with constructs expressing SF2/ASF and Tra2-beta1.

As shown in Figure 7, all exons respond to SF2/ASF and Tra2-beta1, which supports the bioinformatic prediction. It is noticeable that SF2/ASF promotes exon skipping in most cases, and Tra2-beta1 promotes skipping of an exon in the TIAF1 pre-mRNA, which is in contrast to their usual function as splicing activators. This unusual effect of SF2/ASF on tau exon 10 has been previously observed (39). The effect of tra2-beta1 on the POL-B alternative exons was much weaker than on TIAF1, which correlates with the strong binding of tra2-beta1 in vitro to the TIAF1 pre-mRNA and our inability to detect binding of tra2-beta1 to POL-B (Figure 5). Both SF2/ASF and Tra2-beta1 are direct substrates for PP1 and PP1-mediated dephosphorylation that promotes their interaction (3) and it is possible that PyrCer affects exons that are dependent on both factors.

These data indicate that ceramide responsive alternative exons are dependent on splicing regulatory proteins that carry PP1 binding sites. The exons show the strongest response to PSF, suggesting that this factor is central to mediating the signaling between PyrCer and the splicing machinery.
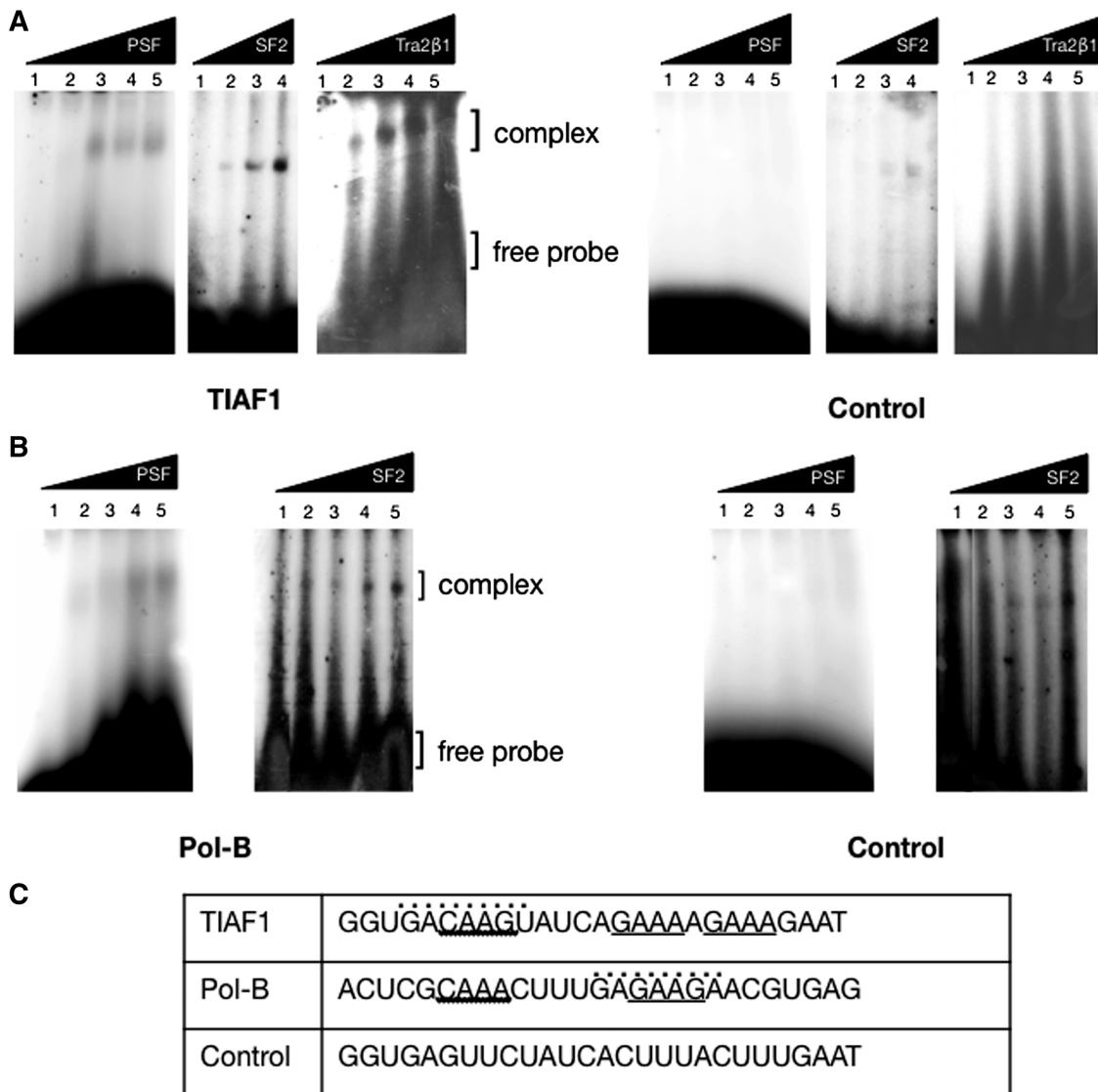
Figure 5. PSF, SF2/ASF and Tra2-beta1 bind to motifs enriched in PyrCer dependent exons. (**A**) Gel retardation assay with TIAF1 and control probes. (**B**) Gel retardation assay with POL-B and control probes. (**C**) Sequence of the RNA probes. The GAAR motif is underlined, the CAAG motif is underlined with zigzag. The SF2/ASF site is indicated by a dotted superscript. The concentration of all oligonucleotides was 0.4 μM in all reactions in a total volume of 10 μl. The protein concentrations for Tra2-beta1 were 0, 2.4, 3.6, 4.8 and 7.2 μM in lanes 1–5, respectively. The concentrations for PSF/SFPQ were 0, 0.5, 1.1, 2.1 and 3.2 μM in lanes 1–5, respectively. The concentration for SF2/ASF was 0, 1.1, 2.8, 4.0 and 5.7 μM and in lanes 1–5, respectively.

DISCUSSION

Role of lipids in RNA metabolism

Lipids have been long known for their role as signaling molecules that are important for human health. Their best-understood mode of action is the regulation of protein phosphorylation by modulating the activity of kinases and phosphatases (40). However, there is emerging evidence that lipids directly interfere with RNA metabolism. For example, high levels of palmitaic acid are toxic for cells, which is mediated through an inter-action with snoRNAs in the cytosol, where snoRNAs are normally not detectable (41). Similar to our findings, different lipids show various degrees of toxicity and RNA association. RNAs were shown to directly bind to membranes where it associates with liquid-ordered rafts (42) and RNA induced silencing complexes (RISC) are associated with endosomal membranes (43,44), suggesting that lipid composition regulates RNA processing complexes. The function of the lipids could be structural by providing scaffolds for protein and RNA assembly as well as catalytic by interfering with the activity of RNA processing enzymes, which was tested here.

In contrast to long-chain ceramides, C6 pyridinium ceramide blocks endogenous protein phosphatase-1 activity

Previously, it was found that short chain D-erythro-C6 ceramide (24) and long-chain D-erythro-C18-ceramide activate PP1 (13) and cause a decrease in SR-protein
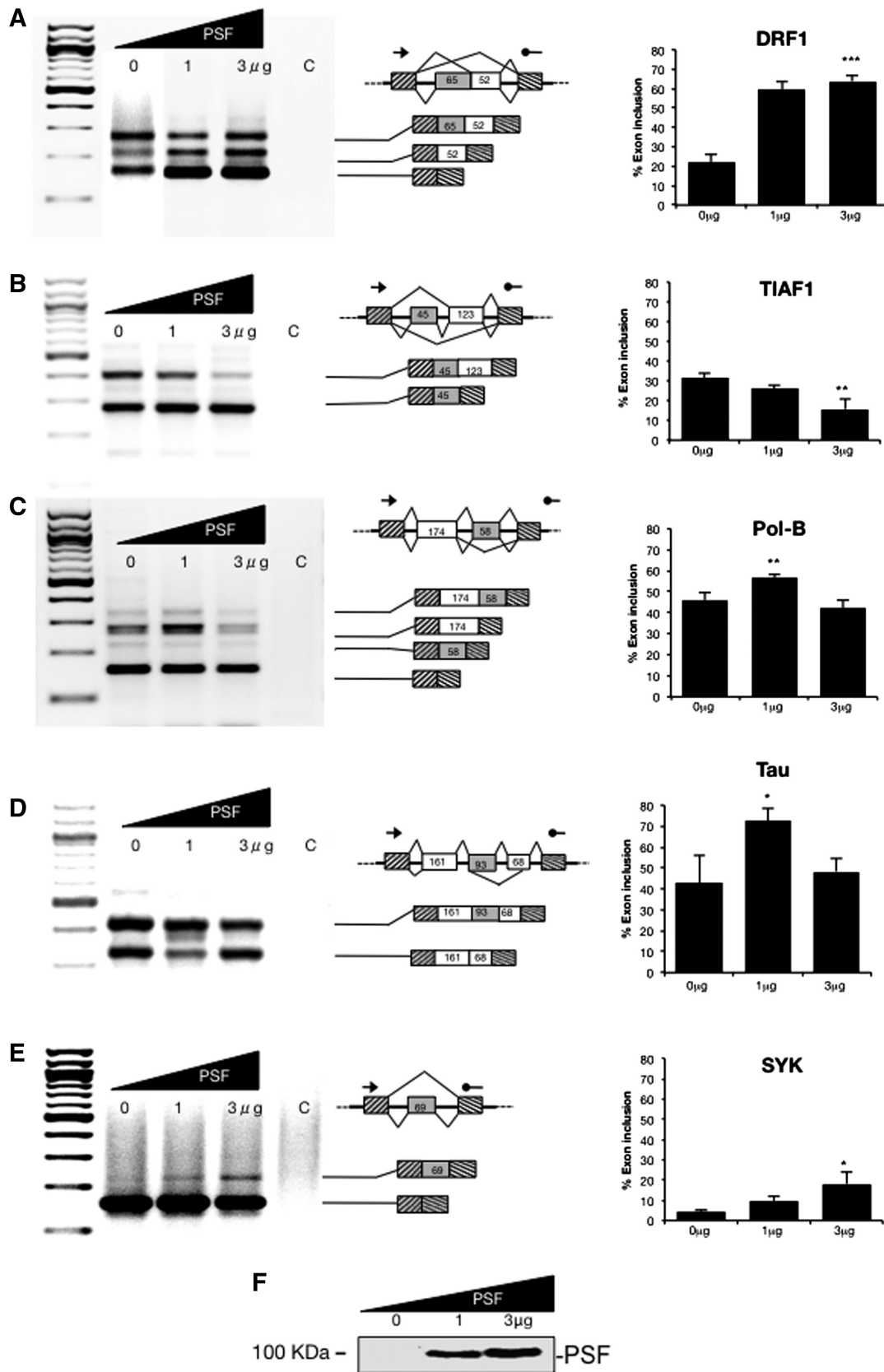
Figure 6. PSF regulates ceramide responsive exons. The reporter genes shown in Figure 2 were co-transfected with a construct expressing PSF (**A–E**). The statistical analysis is shown on the right: n = 4, P = 0.0001, 0.01, 0.009, 0.024, 0.013 for DRF1, TIAF1, POL-B, tau and SYK. F shows the increase of EGFP-PSF protein upon overexpression, detected by an antibody against GFP. Note that no PyrCer was added in these experiments.
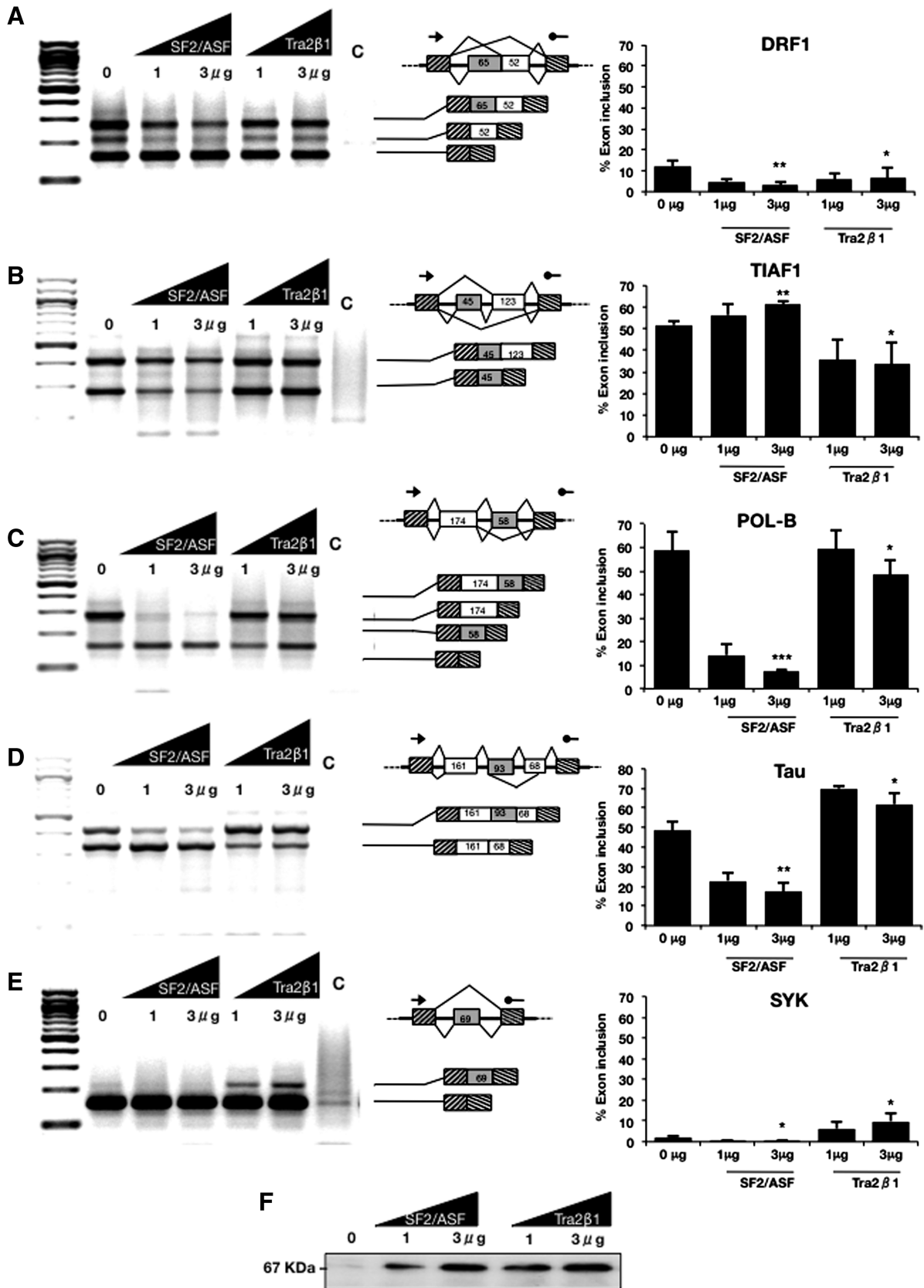
Figure 7. Splicing regulators with a PP1 binding site regulate ceramide responsive exons. The reporter genes shown in Figure 2 were co-transfected with constructs expressing SF2/ASF or Tra2-beta1. RNA was isolated and analyzed by RT-PCR (**A–E**). The statistical analysis of at least three independent experiments is shown on the right. Note that no PyrCer was added in these experiments. (**F**) Detection of GFP-SF2/ASF and GFP-Tra2-beta1 by Western Blot analysis.

phosphorylation. As water-soluble ceramides are used as anti-cancer agents, we tested the effect of the water-soluble derivative PyrCer on PP1 activity. Surprisingly we found that PyrCer inhibits the phosphatase, both when using recombinant proteins and nuclear extract. In agreement with an inhibition of PP1, PyrCer causes an increase of phosphorylation of SF2/ASF, the opposite of its natural derivatives, and the short non-cationic D-erythro-C6 ceramide. Purified PP1 is inhibited starting at $50 \mu M$, whereas proteins in nuclear extract are influenced at $10 \mu M$ C6 pyridinium ceramide. As PP1 is located in protein complexes, it is likely that allosteric effects that interfere with these complexes play a role in blocking the dephosphorylation of splicing factors. We showed that PyrCer is taken up by the cells and found it in PP1 immunprecipitates, which indicates a direct interaction with PP1, rather than a signal that is mediated through other pathways. These differences in PP1 inhibitions have functional consequences, as PyrCer and related short chain ceramides have different effects on alternative splicing: D-e-C$_6$-ceramide changes bcl-x alternative splicing (7), whereas PyrCer has no effect (Sumanasekera, C. *et al*., unpublished data).

The finding that chemically related lipids have opposing effects on PP1 activity and splicing factor phosphorylation indicates that the cell could use lipid modification to control the phosphorylation of PP1 targets, among them splicing factors. Such lipid modifications have been well documented for the glycerophospholipids, where the electric charge of the water-soluble group is subject to modification, as exemplified by the conversion of phosphotidylinositols to negatively charged phosphoinositides that have distinct signaling properties (45).

C6 pyridinium ceramide influences the phosphorylation of splicing factors

We used a mass-spectrometry approach to identify splicing factors that change their phosphorylation due to PyrCer treatment. The rationale was that both PP1 and splicing factor kinases are present in nuclear extract, where they are required for splicing activity (46,47). The screen resulted in the identification of five proteins that had an increase in their phosphorylation upon PyrCer treatment: PSF/SFPQ, SF2/ASF, Tra2-beta1, UAP56 and SAP155. Whereas the first three proteins are known to interact with PP1 and contain an evolutionary conserved binding site for PP1 in their RRMs, UAP56 and SAP155 are not known to directly bind to PP1. However, it was shown that PP1 is directed to SAP155 via an intermediate protein, NIPP-1 (48). It is possible that PyrCer interferes with the PP1-mediated dephosphorylation of SAP155 by blocking catalysis in a NIPP-1/PP1/SAP155 complex.

Using recombinant proteins, we tested the effect on PyrCer on the dephosphorylation of Tra2-beta1 by PP1. We found the PyrCer blocks the dephosphorylation in this system, indicating a direct influence on the phosphatase-substrate complex. Surprisingly, we did not detect a PyrCer-mediated change of phosphorylation in RNA processing proteins that contain a PP1 binding motif in their RRM, such as SRp30c, RBM15b, SFRS11 and ROD1. In *in vitro* assays, SR proteins are often very similar, whereas *in vivo* analysis shows that they have discrete functions (49). Our findings indicate that chemically related lipids can have opposing effects on the phosphorylation and activity of SR proteins, which could contribute to their physiological regulation.

The C6 pyridinium ceramide signal is transduced by PSF/SFPQ, not only SR proteins

A medium-throughput PCR screen revealed several alternative splicing events that are regulated by C6 pyridinium ceramide. All exons identified were cassette exons that were significantly shorter than constitutive exons and were surrounded by weak splice sites. A search for motifs revealed the occurrence of GAAR and CAAR motifs in each exon. Each motif is expected to be present once in every 128 nt by chance, and should occur 2.5 times when all exons are considered. In the regulated exons there are 7 GAAR and 11 CAAG motifs, suggesting that these motifs are 7-fold enriched in C6 pyridinium ceramide-dependent exons. The motifs overlap with predicted PSF, SF2/ASF and Tra2-beta1 binding sites.

The role of these proteins in regulating ceramide-responsive exons was tested by cotransfection experiments and direct protein binding and PSF showed the strongest effect. This was surprising, as PSF was not known to be regulated by ceramide and is not an SR protein, a protein class previously shown to be regulated by ceramides (18).

It was also unexpected that SF2/ASF promoted mostly exon skipping, which is another unusual feature of PyrCer dependent exons. A possible mechanism could be a recruitment of PP1 by SF2/ASF to the pre-mRNA. The overexpression of SF2/ASF could recruit too much PP1 to the pre-mRNA, which would result in aberrant protein:RNA complexes. In agreement with this model, we observed skipping of C6-ceramide dependent exons when PP1 gamma was overexpressed in transfection studies (data not shown).

The stronger effect of PSF on PyrCer dependent exons could indicate that different lipids prefer distinct splicing factors as targets, suggesting that lipid composition could regulate alternative splice site selection *in vivo*.

SUPPLEMENTARY DATA

Supplementary Data are available at NAR Online: Supplementary Figures S1–S7.

REFERENCES

1. Pan,Q., Shai,O., Lee,L.J., Frey,B.J. and Blencowe,B.J. (2008) Deep surveying of alternative splicing complexity in the human transcriptome by high-throughput sequencing. *Nat. Genet.*, **40**, 1413–1415.
2. Tazi,J., Bakkour,N. and Stamm,S. (2009) Alternative splicing and disease. *Biochim. Biophys. Acta*, **1792**, 14–26.
3. Novoyatleva,T., Heinrich,B., Tang,Y., Benderska,N., Butchbach,M.E., Lorson,C.L., Lorson,M.A., Ben-Dov,C., Fehlbaum,P., Bracco,L. *et al.* (2008) Protein phosphatase 1 binds to the RNA recognition motif of several splicing factors and regulates alternative pre-mRNA processing. *Hum. Mol. Genet.*, **17**, 52–70.
4. Shav-Tal,Y., Cohen,M., Lapter,S., Dye,B., Patton,J.G., Vandekerckhove,J. and Zipori,D. (2001) Nuclear relocalization of the pre-mRNA splicing factor PSF during apoptosis involves hyperphosphorylation, masking of antigenic epitopes, and changes in protein interactions. *Mol. Biol. Cell*, **12**, 2328–2340.
5. Shin,C., Feng,Y. and Manley,J.L. (2004) Dephosphorylated SRp38 acts as a splicing repressor in response to heat shock. *Nature*, **427**, 553–558.
6. Xiao,S.H. and Manley,J.L. (1997) Phosphorylation of the ASF/SF2 RS domain affects both protein-protein and protein-RNA interactions and is necessary for splicing. *Genes Dev.*, **11**, 334–344.
7. Chalfant,C.E., Rathman,K., Pinkerman,R.L., Wood,R.E., Obeid,L.M., Ogretmen,B. and Hannun,Y.A. (2002) De novo ceramide regulates the alternative splicing of caspase 9 and Bcl-x in A549 lung adenocarcinoma cells. Dependence on protein phosphatase-1. *J. Biol. Chem.*, **277**, 12587–12595.
8. Ghosh,N., Patel,N., Jiang,K., Watson,J.E., Cheng,J., Chalfant,C.E. and Cooper,D.R. (2007) Ceramide-activated protein phosphatase involvement in insulin resistance via Akt, serine/arginine-rich protein 40, and ribonucleic acid splicing in L6 skeletal muscle cells. *Endocrinology*, **148**, 1359–1366.
9. Ledeen,R.W. and Wu,G. (2008) Nuclear sphingolipids: metabolism and signaling. *J. Lipid Res.*, **49**, 1176–1186.
10. Massiello,A., Salas,A., Pinkerman,R.L., Roddy,P., Roesser,J.R. and Chalfant,C.E. (2004) Identification of two RNA cis-elements that function to regulate the 5′ splice site selection of Bcl-x pre-mRNA in response to ceramide. *J. Biol. Chem.*, **279**, 15799–15804.
11. Senkal,C.E., Ponnusamy,S., Rossi,M.J., Sundararaj,K., Szulc,Z., Bielawski,J., Bielawska,A., Meyer,M., Cobanoglu,B., Koybasi,S. *et al.* (2006) Potent antitumor activity of a novel cationic pyridinium-ceramide alone or in combination with gemcitabine against human head and neck squamous cell carcinomas in vitro and in vivo. *J. Pharmacol. Exp. Ther.*, **317**, 1188–1199.
12. Separovic,D., Saad,Z.H., Edwin,E.A., Bielawski,J., Pierce,J.S., Buren,E.V. and Bielawska,A. (2011) C16-ceramide analog combined with Pc 4 photodynamic therapy evokes enhanced total ceramide accumulation, promotion of DEVDase activation in the absence of apoptosis, and augmented overall cell killing. *J. Lipids*, **2011**, 713867.
13. Chalfant,C.E., Kishikawa,K., Mumby,M.C., Kamibayashi,C., Bielawska,A. and Hannun,Y.A. (1999) Long chain ceramides activate protein phosphatase-1 and protein phosphatase-2A. Activation is stereospecific and regulated by phosphatidic acid. *J. Biol. Chem.*, **274**, 20313–20317.
14. Kishore,S., Khanna,A. and Stamm,S. (2008) Rapid generation of splicing reporters with pSpliceExpress. *Gene*, **427**, 104–110.
15. Beullens,M., Van Eynde,A., Stalmans,W. and Bollen,M. (1992) The isolation of novel inhibitory polypeptides of protein phosphatase 1 from bovine thymus nuclei. *J. Biol. Chem.*, **267**, 16538–16544.
16. Sullards,M.C., Allegood,J.C., Kelly,S., Wang,E., Haynes,C.A., Park,H., Chen,Y. and Merrill,A.H. Jr (2007) Structure-specific, quantitative methods for analysis of sphingolipids by liquid chromatography-tandem mass spectrometry: "inside-out" sphingolipidomics. *Methods Enzymol.*, **432**, 83–115.
17. Pamuklar,Z., Federico,L., Liu,S., Umezu-Goto,M., Dong,A., Panchatcharam,M., Fulerson,Z., Berdyshev,E., Natarajan,V., Fang,X. *et al.* (2009) Autotaxin/lysopholipase D and lysophosphatidic acid regulate murine hemostasis and thrombosis. *J. Biol. Chem.*, **284**, 7385–7394.
18. Massiello,A. and Chalfant,C.E. (2006) SRp30a (ASF/SF2) regulates the alternative splicing of caspase-9 pre-mRNA and is required for ceramide-responsiveness. *J. Lipid Res.*, **47**, 892–897.
19. Karahatay,S., Thomas,K., Koybasi,S., Senkal,C.E., Elojeimy,S., Liu,X., Bielawski,J., Day,T.A., Gillespie,M.B., Sinha,D. *et al.* (2007) Clinical relevance of ceramide metabolism in the pathogenesis of human head and neck squamous cell carcinoma (HNSCC): attenuation of C(18)-ceramide in HNSCC tumors correlates with lymphovascular invasion and nodal metastasis. *Cancer Lett.*, **256**, 101–111.
20. Separovic,D., Bielawski,J., Pierce,J.S., Merchant,S., Tarca,A.L., Bhatti,G., Ogretmen,B. and Korbelik,M. (2011) Enhanced tumor cures after Foscan photodynamic therapy combined with the ceramide analog LCL29. Evidence from mouse squamous cell carcinomas for sphingolipids as biomarkers of treatment response. *Int. J. Oncol.*, **38**, 521–527.
21. Venables,J.P., Klinck,R., Bramard,A., Inkel,L., Dufresne-Martin,G., Koh,C., Gervais-Bird,J., Lapointe,E., Froehlich,U., Durand,M. *et al.* (2008) Identification of alternative splicing markers for breast cancer. *Cancer Res.*, **68**, 9525–9531.
22. Stamm,S. (2002) Signals and their transduction pathways regulating alternative splicing: a new dimension of the human genome. *Hum. Mol. Genet.*, **11**, 2409–2416.
23. Andreadis,A. (2005) Tau gene alternative splicing: expression patterns, regulation and modulation of function in normal brain and neurodegenerative diseases. *Biochem. Biophys. Acta*, **1739**, 91–103.
24. Chalfant,C.E., Ogretmen,B., Galadari,S., Kroesen,B.J., Pettus,B.J. and Hannun,Y.A. (2001) FAS activation induces dephosphorylation of SR proteins; dependence on the de novo generation of ceramide and activation of protein phosphatase 1. *J. Biol. Chem.*, **276**, 44848–44855.
25. Daoud,R., Mies,G., Smialowska,A., Oláh,L., Hossmann,K. and Stamm,S. (2002) Ischemia induces a translocation of the splicing factor tra2-beta1 and changes alternative splicing patterns in the brain. *J. Neurosci.*, **22**, 5889–5899.
26. Patton,J.G., Porro,E.B., Galceran,J., Tempst,P. and Nadal-Ginard,B. (1993) Cloning and characterization of PSF, a novel pre-mRNA splicing factor. *Genes Dev.*, **7**, 393–406.
27. Urban,R.J., Bodenburg,Y., Kurosky,A., Wood,T.G. and Gasic,S. (2000) Polypyrimidine tract-binding protein-associated splicing factor is a negative regulator of transcriptional activity of the porcine p450scc insulin-like growth factor response element. *Mol. Endocrinol.*, **14**, 774–782.
28. Akhmedov,A.T. and Lopez,B.S. (2000) Human 100-kDa homologous DNA-pairing protein is the splicing factor PSF and promotes DNA strand invasion. *Nucleic Acids Res.*, **28**, 3022–3030.
29. Liu,L., Xie,N., Rennie,P., Challis,J.R., Gleave,M., Lye,S.J. and Dong,X. (2011) Consensus PP1 binding motifs regulate transcriptional corepression and alternative RNA splicing activities of the steroid receptor coregulators, p54nrb and PSF. *Mol. Endocrinol.*, **25**, 1197–1210.
30. Hirano,K., Erdodi,F., Patton,J.G. and Hartshorne,D.J. (1996) Interaction of protein phosphatase type 1 with a splicing factor. *FEBS Lett.*, **389**, 191–194.
31. Bailey,T.L. and Elkan,C. (1994) Fitting a mixture model by expectation maximization to discover motifs in biopolymers. *Proc. Int. Conf. Intell. Syst. Mol. Biol.*, **2**, 28–36.
32. Smith,P.J., Zhang,C., Wang,J., Chew,S.L., Zhang,M.Q. and Krainer,A.R. (2006) An increased specificity score matrix for the

prediction of SF2/ASF-specific exonic splicing enhancers. *Hum. Mol. Genet.*, **15**, 2490–2508.

33. Stamm,S., Zhu,J., Nakai,K., Stoilov,P., Stoss,O. and Zhang,M.Q. (2000) An alternative-exon database and its statistical analysis. *DNA Cell Biol.*, **19**, 739–756.

34. Clery,A., Jayne,S., Benderska,N., Dominguez,C., Stamm,S. and Allain,F.H. (2011) Molecular basis of purine-rich RNA recognition by the human SR-like protein Tra2-beta1. *Nat. Struct. Mol. Biol.*, **18**, 443–450.

35. Jiang,Z., Tang,H., Havlioglu,N., Zhang,X., Stamm,S., Yan,R. and Wu,J.Y. (2003) Mutations in tau gene exon 10 associated with FTDP-17 alter the activity of an exonic splicing enhancer to interact with Tra2 beta. *J. Biol. Chem.*, **278**, 18997–19007.

36. Ray,P., Kar,A., Fushimi,K., Havlioglu,N., Chen,X. and Wu,J.Y. (2011) PSF suppresses tau Exon 10 inclusion by interacting with a stem-loop structure downstream of exon 10. *J. Mol. Neurosci.*, **45**, 453–466.

37. Kondo,S., Yamamoto,N., Murakami,T., Okumura,M., Mayeda,A. and Imaizumi,K. (2004) Tra2 beta, SF2/ASF and SRp30c modulate the function of an exonic splicing enhancer in exon 10 of tau pre-mRNA. *Genes Cells*, **9**, 121–130.

38. Peng,R., Dye,B.T., Perez,I., Barnard,D.C., Thompson,A.B. and Patton,J.G. (2002) PSF and p54nrb bind a conserved stem in U5 snRNA. *RNA*, **8**, 1334–1347.

39. Wang,J., Gao,Q.-S., Wang,Y., Lafyatis,R., Stamm,S. and Andreadis,A. (2004) Tau exon 10, whose missplicing causes frontotemporal dementia, is regulated by an intricate interplay of Cis elements and Trans factors. *J. Neurochem.*, **88**, 1078–1090.

40. Wymann,M.P. and Schneiter,R. (2008) Lipid signalling in disease. *Nat. Rev. Mol. Cell Biol.*, **9**, 162–176.

41. Michel,C.I., Holley,C.L., Scruggs,B.S., Sidhu,R., Brookheart,R.T., Listenberger,L.L., Behlke,M.A., Ory,D.S. and Schaffer,J.E. (2011) Small nucleolar RNAs U32a, U33, and U35a are critical mediators of metabolic stress. *Cell Metab.*, **14**, 33–44.

42. Janas,T. and Yarus,M. (2006) Specific RNA binding to ordered phospholipid bilayers. *Nucleic Acids Res.*, **34**, 2128–2136.

43. Siomi,H. and Siomi,M.C. (2009) RISC hitches onto endosome trafficking. *Nat. Cell Biol.*, **11**, 1049–1051.

44. Gibbings,D.J., Ciaudo,C., Erhardt,M. and Voinnet,O. (2009) Multivesicular bodies associate with components of miRNA effector complexes and modulate miRNA activity. *Nat. Cell Biol.*, **11**, 1143–1149.

45. Martin,T.F. (1998) Phosphoinositide lipids as signaling molecules: common themes for signal transduction, cytoskeletal regulation, and membrane trafficking. *Annu. Rev. Cell. Dev. Biol.*, **14**, 231–264.

46. Mermoud,J.E., Cohen,P. and Lamond,A.I. (1992) Ser/Thr-specific protein phosphatases are required for both catalytic steps of pre-mRNA splicing. *Nucleic Acids Res.*, **20**, 5263–5269.

47. Stamm,S. (2008) Regulation of alternative splicing by reversible phosphorylation. *J.Biol. Chem.*, **283**, 1223–1227.

48. Tanuma,N., Kim,S.E., Beullens,M., Tsubaki,Y., Mitsuhashi,S., Nomura,M., Kawamura,T., Isono,K., Koseki,H., Sato,M. *et al.* (2008) Nuclear inhibitor of protein phosphatase-1 (NIPP1) directs protein phosphatase-1 (PP1) to dephosphorylate the U2 small nuclear ribonucleoprotein particle (snRNP) component, spliceosome-associated protein 155 (Sap155). *J. Biol. Chem.*, **283**, 35805–35814.

49. Shepard,P.J. and Hertel,K.J. (2009) The SR protein family. *Genome Biol.*, **10**, 242.